Biosensors and Bioelectronics 41 (2013) 764–770

Contents lists available at SciVerse ScienceDirect

Biosensors and Bioelectronics

journal homepage: www.elsevier.com/locate/bios

Highly sensitive detection of telomerase activity in tumor cells by cascade isothermal signal amplification based on three-way junction and base-stacking hybridization

Yongxi Zhao [a,*], Lin Qi [a], Feng Chen [a], Yue Zhao [a], Chunhai Fan [b]

[a] Key Laboratory of Biomedical Information Engineering of Education Ministry, School of Life Science and Technology, Xi'an Jiaotong University, Xi'an, Shaanxi 710049, PR China
[b] Shanghai Institute of Applied Physics, Chinese Academy of Sciences, Shanghai 201800, PR China

ARTICLE INFO

Article history:
Received 16 August 2012
Received in revised form
21 September 2012
Accepted 2 October 2012
Available online 11 October 2012

Keywords:
Telomerase
Tumor cells
Cascade isothermal signal amplification
Three-way junction
Base-stacking hybridization

ABSTRACT

Herein, We report a simple and highly sensitive telomerase activity assay that integrates two consecutive isothermal signal amplification processes, namely, three-way junction triggered DNA-machine (3WJ-DNAM), and base-stacking hybridization assisted "biological circuit" DNA-machine (BSHBC-DNAM). In the presence of telomerase, the 3WJ are formed by the hybridization between the telomerase product and 3WJ-probes (3WJ-primer and 3WJ-template), which will initiate an autonomous 3WJ-DNAM by multiple processes of replication, nicking, and strand displacement, continuously generating short oligonucleotides as "triggers". These "triggers" will then provide additional stability for another two primers with a shared 5-bp complementary sequence at each 3′-end via base-stacking hybridization. And the BSHBC-DNAM are subsequently carried out by the strand-displacement induced circular utilization of "Trigger". Eventually, the single-stranded DNA (ssDNA) is generated in large quantities, and a significant fluorescence enhancement is observed due to the hybridization between the ssDNA and molecular beacons (MBs). In this way, per telomerase-mediated elongation event is efficiently and specifically converted into the greatly amplified fluorescence signals. This novel sensing strategy permits measurement of telomerase activity in cell extracts over the range of 3–5000 Hela cells, which is comparable or even superior to most previously reported methods. Using somatic and tumor cell lines, the selectivity and generality of the assay are investigated with satisfactory results. Furthermore, the inhibition effect of 3′-azido-3′-deoxythymidine (AZT) is also investigated, indicating its excellent performance in telomerase inhibitor screening.

1. Introduction

Telomerase is a specialized ribonucleoprotein (RNP) reverse transcriptase that remediates chromosomal shrinkage resulting from the "end-replication" problem by using its intrinsic RNA subunit as template for the addition of $(TTAGGG)_n$ onto the 3′-end of the human chromosomes (Morin, 1989; Blackburn, 1991; Cohen et al., 2007). It is well documented that telomerase is over-expressed in the majority of cancer cells, whereas it is absent or repressed in most somatic cells, implying that telomerase is associated with tumorigenesis (Kim et al., 1994; Shay and Bacchetti, 1997; Greider, 1998). Consequently, the identification of telomerase activity and their potential inhibitors are not only valuable for fundamental biochemical research in elucidating the relationship between telomerase and cancer, but also significant for clinical tumor diagnosis and telomerase-targeted drug discovery (Shay and Wright, 2002; Mergny et al., 2002).

Over the past decades, owing to extremely high sensitivity and wide detection range, a polymerase chain reaction (PCR) based telomeric repeat amplification protocol (TRAP) has been widely employed for the estimation of telomerase activity (Kim et al., 1994; Kim and Wu, 1997). However, the original TRAP assay is time-consuming, not easily quantified, susceptible to PCR-related artifacts, and difficult for screening telomerase inhibition (Zhou and Xing, 2012; De Cian et al., 2007; Niemeyer et al., 2005). Furthermore, some potential interferents in real samples may inhibit the activity of Taq polymerase, resulting in a false negative result (Zhou et al., 2008). Finally, the requirement for high-precision thermal cycling and skilled operators in PCR technique makes it high cost and difficult to execute point-of-care analysis. Subsequently, some modified approaches have been developed for circumventing the aforementioned drawbacks (Xiao et al., 2010; Hou et al., 2001; Wege et al., 2002; Öztürk et al., 2008; Eskiocak et al., 2007; Atha et al., 2003). Unfortunately, PCR-derived

* Corresponding author. Tel./fax: +86 29 82663454.
E-mail address: yxzhao@mail.xjtu.edu.cn (Y. Zhao).

0956-5663/$ - see front matter © 2012 Elsevier B.V. All rights reserved.
http://dx.doi.org/10.1016/j.bios.2012.10.009

issues still limit their practical applications. Alternatively, many PCR-free telomerase assays have been established (Zhou et al., 2008; Yang et al., 2011; Wu et al., 2012; Shao et al., 2008; Wang et al., 2012a; Wang et al., 2012b; Xiao et al., 2004; Li et al., 2011; Niazov et al., 2004). Nevertheless, most of them have the disadvantages of being expensive, lacking simplicity, suffering from insufficient sensitivity and narrow detection range, or the requirement for elaborate instruments. Although some assays can offer the impressive sensitivity, multi-step and time-consuming processes caused by immobilization of telomerase substrate (TS) on solid supports or other nanoparticles, relatively poor salt stability of some nanomaterial as signal transducer/amplifier, variability from synthesis and labeling procedures of nanoprobes present some limitations for their practical implementation (Wu et al., 2012; Wang et al., 2012b; Sharon et al., 2010).

Due to their inherited advantages such as simplicity, sensitivity, high-throughput ability and ease of automation, several impressive fluorescence-based approaches have been developed for analyzing telomerase activity (Zhang et al., 2012; Zuo et al., 2011; Wang et al., 2012a; Peng et al., 2012; Ding et al., 2010). These strategies avoid the PCR-derived problems and requirement for gel analysis in TRAP assay, permitting the measurement of telomerase activity from cell extracts in a simple and isothermal way. In addition to the narrow detection ranges, the sensitivities of assays based on signal amplification are comparable to the PCR-based detection and better than that of most previously reported PCR-free approaches (Zuo et al. 2011; Wang et al., 2012a; Wang et al., 2012b; Peng et al. 2012; Ding et al., 2010). Overall, the above fluorescence-based approaches make significant contributions to telomerase activity assay, however, the development of a novel isothermal amplification strategy for further improvement of the analytical performances including sensitivity, detection range, etc. is still in urgent need.

Among a variety of nucleic acid amplification strategies, autonomous DNA-machine by multiple processes of replication, nicking, and strand displacement has attracted considerable attention for its excellent isothermal amplification capability (Li et al., 2008; Shlyahovsky et al., 2007). The whole operations proceed at constant temperature using a polymerase possessing strand displacement activity, and a nicking endonuclease that can cleave ssDNA in a duplex with specific sequence, which appears to be less affected by inhibitory compounds in clinical samples than PCR-based assays (Niemz et al., 2011), More recently, some modified DNA-machines, such as cascade signal amplification (Ma et al., 2012), circular double-assisted signal amplification (Zhou et al., 2011), and exponential amplification reaction (EXPAR) (Zhang and Zhang, 2012; Jia et al., 2010) have been developed for the detection of protein, DNA, and MicroRNA, offering remarkable or even exponential signal amplification and a wide detection range.

Inspired by their works, to further improve the sensitivity and broaden the detection range of the telomerase activity assay, we have developed for the first time a three-way junction triggered DNA-machine (3WJ-DNAM), and a base-stacking hybridization assisted "biological circuit" DNA-machine (BSHBC-DNAM), and elaborately integrated the two isothermal signal amplification strategies into a fluorescence sensing system for screening telomerase activity and its inhibitors.

2. Experimental

2.1. Reagents and materials

Klenow Fragment (3′→5′ exo-) and the Nt.BbvCI were purchased from New England Biolabs Ltd. (Beijing, China). The RNase Inhibitor was obtained from Biyuntian (Nantong, China). The deoxynucleotide triphosphates (dNTPs) were obtained from TaKaRa Biotechnology Co. Ltd. (Dalian, China). The 1 × CHAPS Lysis Buffer (0.5% CHAPS, 10 mM Tris–HCl, pH = 7.5, 1 mM $MgCl_2$, 1 mM EGTA, 5 mM β-mercaptoethanol, 0.1 mM PMSF, 10% glycerol) was purchased from Millipore (Bedford, MA). HeLa cells were obtained from Chinese Academy of Medical Sciences. And the 3′-azido-3′-deoxythymidine (AZT) was purchased from Sigma-Aldrich. All other reagents were used directly without further purification. The Milli-Q water (resistance > 18.2 MΩ) used for solution preparation and reaction was RNase-free. All oligonucleotides used in this work were synthesized and HPLC purified by Sangon Biotechnology Co., Ltd (Shanghai, China). Their sequences were shown in Table S1.

2.2. Telomerase extension reaction

Telomerase extracts from Hela cells or other cells were first diluted with 1 × CHAPS lysis buffer. And 2 μL of the diluted telomerase extracts equivalent to a series of respective number of cells were added into the telomerase extension reaction buffer containing 20 mM Tris–HCl, 1.5 mM $MgCl_2$, 1 mM EGTA, 63 mM KCl, 0.05% Tween 20, 0.2 mM dNTPs, and 150 nM TS-primer (pH = 7.9), with the total volume of 10 μL. The solution was incubated at 30 °C for 60 min.

2.3. Telomerase detection by cascade isothermal signal amplification

The resulting solution of telomerase extension reaction was mixed with 10 nM 3WJ-primer (−2), 10 nM 3WJ-template, 50 nM primer 1(19), 50 nM primer 2, 100 nM MBs, 0.1 U/μL Klenow Fragment, 0.2 U/μL Nt.BbvCI, and 0.2 mM dNTPs in 100 μL 1 × NEB buffer 2 and incubated at 37 °C for 100 min prior to fluorescence measurements. For the control experiment, telomerase extracts from 2500 Hela cells were heat-treated at 90 °C for 20 min before use.

3. Results and discussion

3.1. Principle of the telomerase assay

The whole telomerase detection illustrated in Scheme 1 can be divided into two steps, namely, telomerase extension reaction and cascade isothermal signal amplification which integrates a 3WJ-DNAM and the BSHBC-DNAM. And five different oligonucleotides containing TS-primer, 3WJ-probes, and two primers (primers 1 and 2) are involved in this proposed sensing strategy. In details, there are five and three domains in 3WJ-probes and two primers, respectively. The domain I in 3WJ-template is designed to be complementary to a part of the TS-primer (red). The domain II (orange) of 3WJ-probes and domain VII (brown) of two primers only possess 7-bp and 5-bp long complementary sequences, respectively. The domain IV in 3WJ-primer contains two bases complementary to 3′-end of TS-primer (yellow). The domain V in 3WJ-primer including three TCCCAA repeats is designed to be complementary to the three AGGGTT repeats on telomerase product adjacent to the 3′-end of TS-primer (green). The domain III (blue) in 3WJ-template and domain VIII (purple) in primer 2 serve as a "track" for autonomous DNA-machine. Moreover, the 3′-end of 3WJ-template is modified with phosphate (marked with "P") to inhibit nonspecific amplification (Murakami et al., 2012). In the presence of telomerase and dNTPs, the telomerase extension reaction is carried out by adding AGGGTT repeats to the 3′-end of TS-primer to generate telomerase product, whose amount is proportional to the telomerase activity

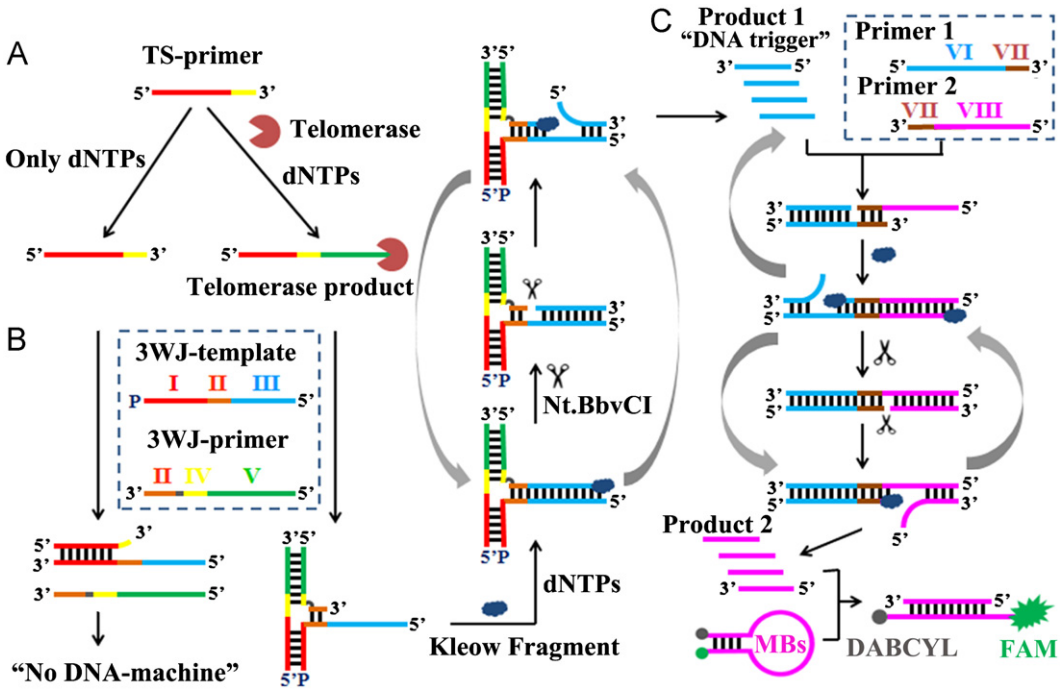

Scheme 1. Schematic illustration of telomerase activity assay by cascade isothermal signal amplification: (A) telomerase extension reaction step, (B) 3WJ-DNAM and (C) BSHBC-DNAM.

(Zhou and Xing, 2012). The telomerase product could then selectively hybridize with 3WJ-probes in close proximity to form a stable 3WJ. The two "A" bases adjacent to domain II in 3WJ-primer form an unpaired nucleotide bulge (gray) in the junction which can improve the thermodynamic stability of the 3WJ (Kong et al., 2011). Subsequently, in the presence of Klenow Fragment and dNTPs as "fuel substrate", a 3WJ-DNAM including replication, nicking, and strand displacement are repeated continuously through the 3′-end of 3WJ-primer, generating a great deal of short oligonucleotides (product 1) as "Trigger". The displaced "Trigger" is complementary to the domain VI in primer 1 which can provide additional stability to the short 5-bp duplex of the two primers, namely base-stacking hybridization. It describes a phenomenon that two or more shorter oligonucleotides hybridize to a longer complementary ssDNA in a contiguous tandem can strongly stabilize the short DNA duplex through stacking interaction (Lu et al., 2011). As a result, the 3′-end of primer 1 will initiate another DNA-machine by using primer 2 as a template. The displaced oligonucleotides (product 2) as reporter units will then hybridize with numerous MBs, disrupting the hairpin structure and leading to the significant fluorescence restoration. Meanwhile, 3′-end of primer 2 will also be extended, resulting in the displacement and circular utilization of "Trigger". This turns the linear DNA-machine into an automatic "biological circuit" DNA-machines. Eventually, per telomerase extension event can be successfully converted into a dramatically amplified fluorescence signal by 3WJ-DNAM coupled with BSHBC-DNAM. On the contrary, in the absence of target telomerase, the 3WJ and the heterodimer of two primers cannot exist stably under the reaction temperature due to the shorter complementary sequences in domains II, IV, and VII. Therefore, nearly no amplification can be triggered, which ensures a low background signal.

3.2. Investigation of 3WJ-DNAM

The hybridization site between telomerase product and 3WJ-probes might play a key role in the performance of 3WJ-DNAM. To directly and simply evaluate the effect of the hybridization sites on the signal amplification efficiency, an ssDNA containing the sequence of TS primer and five "AGGGTT" repeats was commercially synthesized for simulating telomerase product, and the 5′-end of 3WJ-template was modified for directly obtaining the resultant product 2 which could hybridize with MBs (Scheme S1). The four different hybridization sites between telomerase product and 3WJ-probes are depicted in Fig. 1A, respectively. Hybridization site "0" represents that the three AGGGTT repeats on telomerase product adjacent to TS-primer are perfectly complementary to 5′-end of 3WJ-primer, and the sequence of TS-primer are perfectly complementary the 3' end of 3WJ-template. While hybridization sites "−2", "−4", and "−6" mean that there are 2, 4, and 6 bases at the 3′-end of TS primer complementary to 3WJ-primer, instead of 3WJ-template. One can imagine that without telomerase product, hybridization site "0" will lead to a significant background signal because the 3′-end of TS-primer fully hybridizing with 3WJ-template can be directly extended by Klenow Fragment to trigger the DNA-machine. As shown in Fig. 1B, we observed extremely high background fluorescence for the hybridization site "0", which was even higher than the fluorescence response caused by the telomerase product. For the hybridization sites "−2","−4", and "−6", all of them exhibited a low background signal, which indicate that with several bases noncomplementary to the 3WJ-template, the 3WJ-DNAM triggered by 3′-end of TS primer can be efficiently eliminated in the absence of telomerase product. In addition, the extremely low background signal of the 3WJ-DNAM might also be attributed to the following reasons. First, the shorter duplex between the 3WJ-probes as well as the shorter duplex between 3WJ-primer and TS-primer avoid the formation of the 3WJ for initiating the 3WJ-DNAM. Second, the TS-primer complementary to the upstream sequence of 3WJ-template can lower the probability of a single nucleotide triggered nonspecific amplification (Qian et al., 2012). Moreover, the 3WJ-template is blocked by phosphate at the 3′-end which can further reduce the nonspecific amplification from the 3WJ-template itself. However,

with more bases on the 3′-end of TS-primer complementary to 3WJ-primer rather than 3WJ-template, a slowly increasing tendency of the background signal was also observed. This might be due to the fact that more bases on 3′-end of TS primer complementary to 3WJ-pimer will provide the higher thermodynamic stability for the formation of 3WJ without telomerase product, which further increases nonspecific amplification. In the presence of telomerase product, the hybridization sites "−2","−4", and "−6" displayed the remarkable fluorescence responses, while hybridization site "0" had a relatively lower fluorescence signal. This is probably because that although the 7-bp complementary sequence between the 3WJ-primer and 3WJ-template is able to force the three TCCCAA repeats on the 5′-end of 3WJ-primer to selectively hybridize with the three AGGGTT repeats adjacent to the 3′-end of TS-primer for forming a stable 3WJ-strutcure, there is still a small probability for other hybridizations between 3WJ-primer and telomerase products owing to shorter complementary sequence (7-bp) between 3WJ-probes, and more repeats on telomerase product, which will affect the signal amplification, especially for hybridization site "0". Whereas the special design using the several bases on 3′-end of TS-primer complementary to 3WJ-pimer might effectively solve this problem and consequently improve the sensitivity. Eventually, hybridization site "−2" was chosen for subsequent investigations as fluorescence enhancement ($(F-F_0)/F_0$) was maximized here.

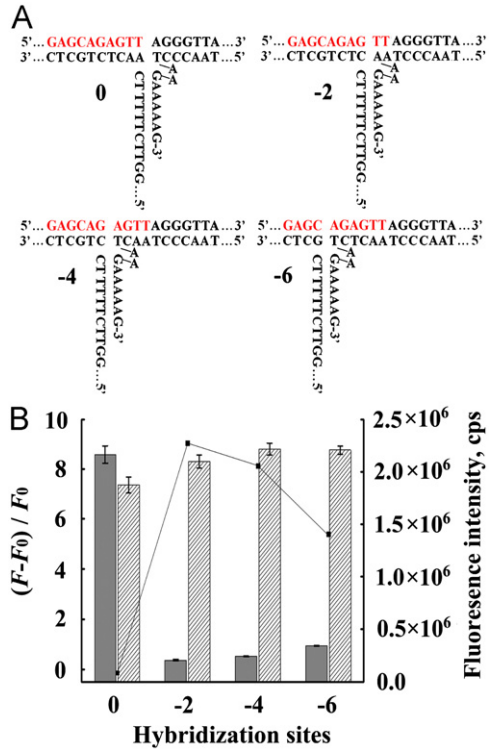

Fig. 1. (A) Depiction of the four different hybridization sites between telomerase product and 3WJ-probes. (B) Effects of the different hybridization sites on the performance of 3WJ-DNAM by using 10 nM 3WJ-probes. The gray and light bars represent the fluorescence intensity at 518 nm in the presence of 10 nM TS-primer (F_0) and 10 nM telomerase product (F), respectively. The line shows the fluorescence enhancement ($(F-F_0)/F_0$) of each hybridization site. The error bars denote the standard deviations for measurements taken from three independent experiments.

3.3. Evaluation of BSHBC-DNAM

The longer duplex between "Trigger" and primer 1 might provide more additional stability for the 5-bp complementary sequence between primers 1 and 2 through contiguous stacking hybridization. However, too long duplex may also prolong the time of "Trigger" displacement, resulting in the poor amplification efficiency. Therefore, using the commercially synthesized "Trigger", the effect of the duplex length over a range from 13-bp to 21-bp on the sensing performance was examined, and the experimental results confirm the above hypothesis (shown in Fig. S1A). In view of the maximum fluorescence enhancement, the 19-bp duplex between "Trigger" and primer 1 was used for the subsequent investigation.

The effect of the concentration of two primers at the molar ratio of 1:1 on the sensing performance was also investigated using a fixed concentration of "Trigger", namely 10 nM. As shown in Fig. S1B, with the increasing concentrations of the two primers, the fluorescence response dramatically enhanced in the presence of "Trigger"; however, the background fluorescence only slightly increased in the negative control. Finally, 100 nM of primers 1 and 2 was selected. In principle, the BSHBC-DNAM will offer more rapid and efficient amplification than previously reported conventional DNA-machines. To confirm this, the conventional DNA-machine was subsequently performed by using our designed primer and template in the same experimental conditions as those used in previous works. It was clearly seen in the inset of Fig. S1B that the proposed DNA-machine resulted in a much higher fluorescence enhancement than that of the conventional DNA-machine, indicating the excellent amplification efficiency of the BSHBC-DNAM. Additionally, it is worthwhile to point out that the two separated primers with only 5-bp duplex can

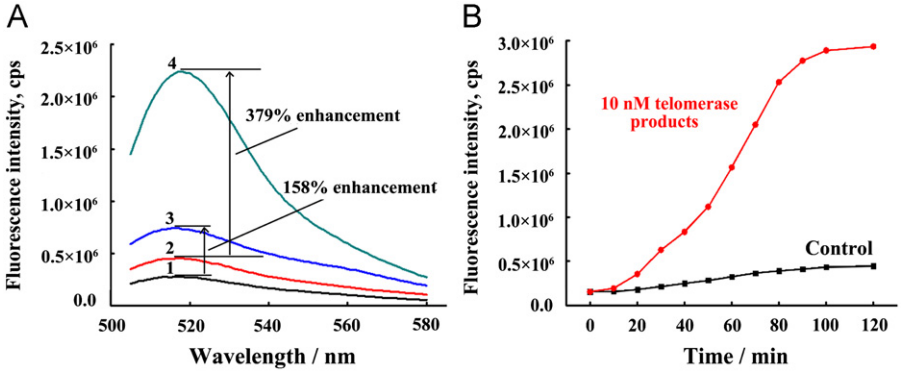

Fig. 2. (A) Comparison of the amplification efficiency of 3WJ-DNAM and cascade isothermal amplification strategy: (1) 10 nM TS-primer and 10 nM 3WJ-probes; (2) 10 nM TS-primer, 10 nM 3WJ-probes, and 100 nM of primer 1 and 2; (3) 5 nM TS-primer, 5 nM telomerase product, and 10 nM 3WJ-probes; (4) 5 nM TS-primer, 5 nM telomerase product, 10 nM 3WJ-probes, and 100 nM of two primers. (B) Time-dependent fluorescence responses of the cascade amplification strategy in the presence of 10 nM telomerase product and 10 nM TS-primer, respectively.

effectively inhibit the nonspecific amplification caused by uncontrolled self-folding in conventional DNA-machines which integrating the sequence of primer and template into one ssDNA (Li et al., 2008; Shlyahovsky et al., 2007).

3.4. Cascade isothermal signal amplification

The amplification capability of the sensing strategy was evaluated and the results are depicted in Fig. 2A. Compared with the background signal of 10 nM TS-primer, the cascade signal amplification strategy resulted in a significant fluorescence enhancement ((379 ± 18)%) upon addition of 5 nM telomerase product and 5 nM TS-primer, whereas a lower fluorescence enhancement ((158 ± 13)%) was obtained by only using 3WJ-DNAM.

Moreover, the reaction time was also optimized. As can be seen in Fig. 2B, the fluorescence response quickly increased with the increasing reaction time, and then leveled off at 100 min in the presence 10 nM telomerase product. Finally, 100 min was chosen for this sensing system, which can rival all of fluorescence signal amplification assays.

3.5. Feasibility verification of the sensing system for real sample by gel electrophoresis

To further confirm the feasibility of the telomerase assay for real sample, a non-denaturating polyacrylamide gel (PAGE) was first employed to analyze the resultant products of 3WJ-structhre triggered DNA-machine (lane 1 and 2) and the cascade signal amplification strategy (lane 3 and 4), respectively (Fig. 3). As depicted in Fig. 3, in the absence of telomerase, a single clearly visible band was present in lane 1 and 3, respectively, indicating the complex formed by the hybridization between TS-primer and 3WJ-template. Upon addition of telomerase extracts from 5000 Hela cells, the respective band in lane 2 and 4 appeared at the molecular weight corresponding to 3WJ, which confirmed that TS-primer was extended by telomerase in real samples, and subsequently formed the stable 3WJ with 3WJ probes. Furthermore, the new bands with a faster migration speed were observed in lane 2 and 4, which are most likely to be product 1 of the 3WJ-DNAM and the product 2 of the BSHBC-DNAM, respectively. In lane 4, a band of approximately 60 bases was also observed, which was corresponding to base-stacking assisted stable duplex of primer 1, primer 2 and "Trigger". The results clearly demonstrate that the novel telomerase assay can be readily applied to the measurement of telomerase activity in real samples.

3.6. Detection of telomerase activity in Hela cells extracts

The concentration of TS-primer is an important factor for ensuring efficient telomerase extension reaction, which will ultimately affect the sensitivity of the novel telomerase assay. Therefore, the effect of TS-primer concentration was evaluated using a fixed telomerase extracts from telomerase-positive 5000 Hela cells. Fig. S2 shows the variance of fluorescence intensity in

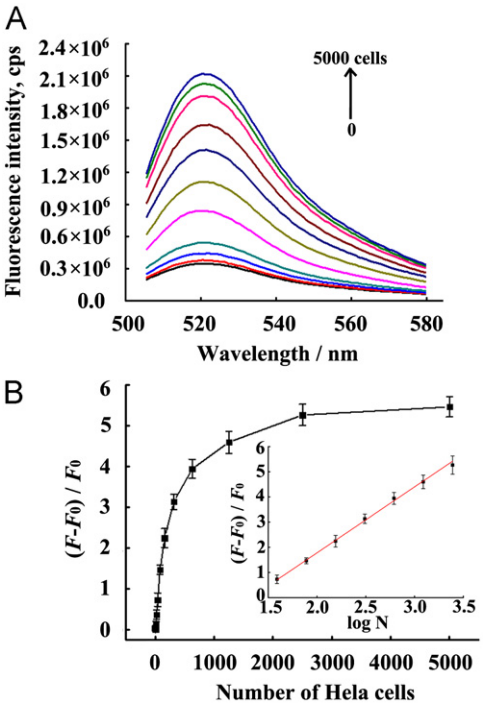

Fig. 4. Cascade isothermal amplified fluorescence detection of telomerase extracts from Hela cells: (A) fluorescence emission spectra in response to telomerase extracts from different numbers of Hela cells. (B) The relationship between the fluorescence enhancement and the cell numbers. The inset shows the linear relationship between the fluorescence enhancement and the logarithm of cell numbers.

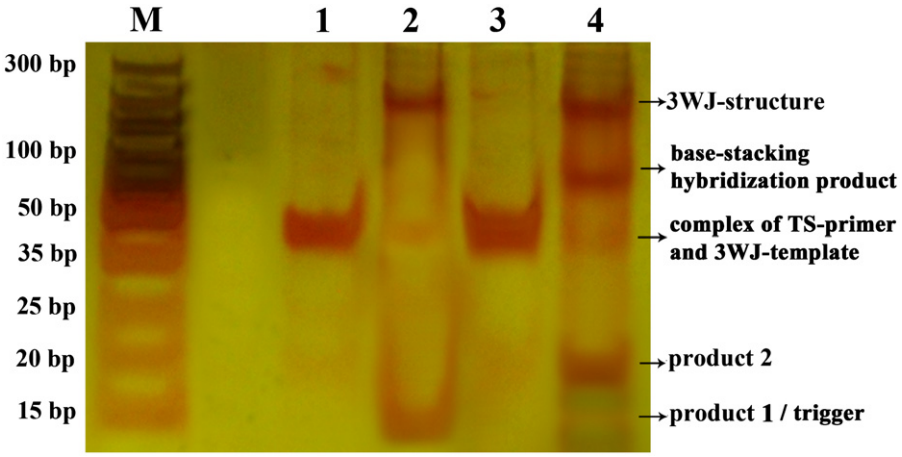

Fig. 3. Non-denaturing PAGE analysis of the products generated by 3WJ triggered DNA machine in the absence (lane 1) and presence (lane 2) of telomerase extracts from 5000 Hela cells, as well as cascade isothermal amplification strategy in the absence (lane 3) and presence (lane 4) of telomerase extracts from 5000 Hela cells, respectively. "M" represents the DNA ladder marker.

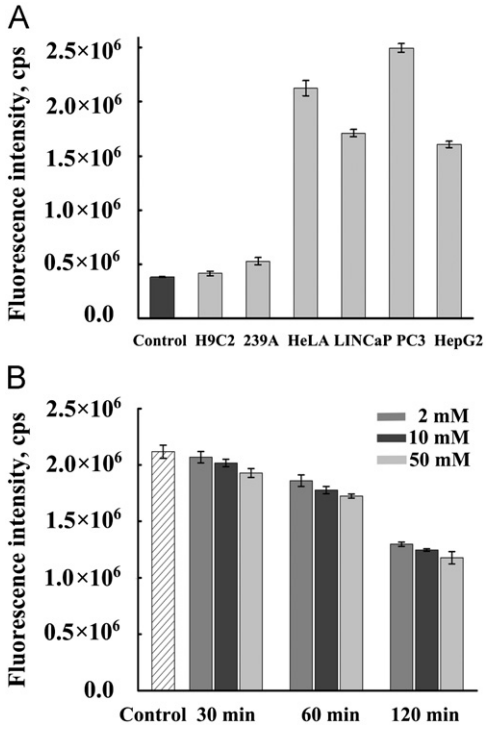

Fig. 5. (A) Fluorescence responses of this sensing system to the telomerase extracts from 2500 cells of different kinds of cell lines and the heat-inactivated telomerase extracts from 2500 Hela cells (control). (B) Inhibition of telomerase activity in extracts from 2500 Hela cells by different concentrations of AZT.

the absence and presence of telomerase with the concentration of TS-primer, respectively. Finally, 150 nM TS-primer was selected for telomerase activity detection.

Fig. 4A depicts the fluorescence emission spectra of the sensing system in response to cell extracts from different number of Hela cells. The fluorescence intensities enhanced quickly when the number was raised from 0 to 5000. Fig. 4B shows the relationship between the fluorescence enhancement at 518 nm and the cell numbers. The inset of Fig. 4B depicts the linear relationship between fluorescence enhancement and the logarithm of cells numbers from 39 to 2500. The detection limit, calculated as three times the signal-to-noise ratio, was estimated to be 3 Hela cells. To our knowledge, the sensitivity is comparable or even superior to most previously reported methods (shown in Table S2). Furthermore, it should be noted that the detection range in our assay is wider than the recently described fluorescence amplification approaches (Wang et al., 2012a, b; Ding et al., 2010). We also measured the telomerase activity in Hela cell extracts by using 3WJ-DNAM only (shown in Fig. S3). Without the BSHBC-DNAM, a significantly poorer detection limit of only 40 cells was observed, further confirming the powerful signal amplification capability of the present sensing system.

To assess the reproducibility of the present sensing system, telomerase activity of extracts from 78 and 625 Hela cells were repeatedly measured, and the relative standard deviation (RSD) obtained are 4.76% and 3.15%, respectively ($n=3$), indicating its great reproducibility.

3.7. Selectivity and generality

Two somatic and four tumor cell lines were used to validate the selectivity and generality of our assay. It is well known that heat can destroy the essential RNA template and reverse transcriptase protein of telomerase. And Fig. 5A shows an obvious decrease in fluorescence signal nearly down to background level for the heat-inactivated Hela cells extract, implying that the signal response is only dependent on telomerase activity. Furthermore, only a slight fluorescence enhancement was observed for two somatic cells extracts, whereas tumor cells extracts resulted in a significant fluorescence enhancement. The difference in the fluorescence response is attributed to the diversity of telomerase expression in different tumor cell lines. These results indicate the high selectivity and general ability of this novel telomerase assay as well as its great potential for further application in clinical tumor samples.

3.8. Inhibition assay

Using AZT as a model inhibitor, the validity of the sensing system in screening the inhibition of telomerase was evaluated. As shown in Fig. 5B, the fluorescence intensities decreased gradually with the increase of AZT concentration and incubation time, suggesting the potential application of the developed assay for studies of telomerase inhibition and telomerase-targeted drug discovery.

4. Conclusion

In summary, we have developed for the first time a cascade isothermal signal amplification strategy that integrates 3WJ-DNAM with BSHBC-DNAM for simple and highly sensitive fluorescence detection of telomerase activity in extracts from cancer cells. Compared with the existing assays based on TS-primer conjugated to nanoparticles, the electrodes or other solid supports, telomerase elongation reaction in our proposed approach is carried out in homogeneous solution, which will avoid the steric hindrance of these solid supports, thereby greatly enhancing the reaction efficiency. Moreover, TS-primer, 3WJ-probes, two primers, and MB are used in the current sensing system, which not only ensure a dramatically low background fluorescence in the absence of target telomerase, but also afford a facile way for converting per telomerase-mediated elongation event into the greatly amplified fluorescence signals. In addition, it is worthwhile to point out that the isothermal operation and simple fluorescence output eliminate the requirement for high-precision thermal cycling and gel analysis in TRAP assays. By using the novel cascade DNA-machines, the telomerase activity in cell extracts down to 3 Hela cells can be detected with an improved detection range up to 5000 Hela cells, which is comparable with or even superior to most previously reported telomerase assays. The entire time needed for our approach is 3 h, which can rival all of fluorescence signal amplification assays and is much faster than conventional TRAP assays. Further investigations have indicated that the proposed sensing system enable simple, highly sensitive, reliable and reproducible measurement of telomerase activity and its inhibitor, and can be extended to detect telomerase activity from other tumor cells. In view of attractive analytical characteristics and distinct advantages, the developed telomerase assay is expected to extend its potential application in point-of-care diagnostics of clinical tumor and telomerase-targeted drug discovery.

Acknowledgments

This research was financially supported by the National Natural Science Foundation of China (21005059).

Appendix A. Supporting information

Supplementary data associated with this article can be found in the online version at: http://dx.doi.org/10.1016/j.bios.2012.10.009.

References

Atha, D.H., Miller, K., Sanow, A.D., Xu, J., Hess, J.L., Wu, O.C., Wang, W., Srivastava, S., Highsmith, W.E., 2003. Electrophoresis 24, 109–114.

Blackburn, E.H., 1991. Nature 350, 569–573.

Cohen, S.B., Graham, M.E., Lovrecz, G.O., Bache, N., Robinson, P.J., Reddel, R.R., 2007. Science 315, 1850–1853.

De Cian, A., Cristofari, G., Reichenbach, P., De Lemos, E., Monchaud, D., Teulade-Fichou, M.P., Shin-ya, K., Lacroix, L., Lingner, J., Mergny, J.L., 2007. Proceedings of the National Academy of Sciences of the United States of America 104, 17347–17352.

Ding, C., Li, X., Ge, Y., Zhang, S., 2010. Analytical Chemistry 82, 2850–2855.

Eskiocak, U., Ozkan-Ariksoysal, D., Ozsoz, M., Öktem, H.A., 2007. Analytical Chemistry 79, 8807–8811.

Greider, C.W., 1998. Proceedings of the National Academy of Sciences of the United States of America 95, 90–92.

Hou, M., Xu, D., Björkholm, M., Gruber, A., 2001. Clinical Chemistry 47, 519–524.

Jia, H., Li, Z., Liu, C., Cheng, Y., 2010. Angewandate Chemie International Edition 49, 5498–5501.

Kim, N.W., Piatyszek, M.A., Prowse, K.R., Harley, C.B., West, M.D., Ho, P.L., Coviello, G.M., Wright, W.E., Weinrich, S.L., Shay, J.W., 1994. Science 266, 2011–2015.

Kim, N.W., Wu, F., 1997. Nucleic Acids Research 25, 2595–2597.

Kong, R.M., Zhang, X.B., Zhang, L.L., Huang, Y., Lu, D.Q., Tan, W., Shen, G.L., Yu, R.Q., 2011. Analytical Chemistry 83, 14–17.

Li, D., Wieckowska, A., Willner, I., 2008. Angewandate Chemie International Edition 120, 3991–3995.

Li, Y., Li, X., Ji, X., 2011. Biosensors and Bioelectronics 26, 4095–4098.

Lu, Z., Duan, D., Cao, R., Zhang, L., Zheng, K., Li, J., 2011. Chemical Communications 47, 7452–7454.

Ma, C., Zhao, C., Ge, Y., Shi, C., 2012. Clinical Chemistry 58, 384–390.

Mergny, J.L., Riou, J.F., Mailliet, P., Teulade-Fichou, M.P., Gilson, E., 2002. Nucleic Acids Research 30, 839–865.

Morin, G.B., 1989. Cell 59, 521–529.

Murakami, T., Sumaoka, J., Komiyama, M., 2012. Nucleic Acids Research 40, e22.

Niazov, T., Pavlov, V., Xiao, Y., Gill, R., Willner, I., 2004. Nano Letters 4, 1683–1687.

Niemeyer, C.M., Adler, M., Wacker, R., 2005. Trends in Biotechnology 23, 208–216.

Niemz, A., Ferguson, T.M., Boyle, D.S., 2011. Trends in Biotechnology 29, 240–250.

Öztürk, K., Durusoy, M., Pişkin, E.J., 2008. Bioactive and Compatible Polymers 23, 579–593.

Peng, L., Zhu, Z., Chen, Y., Han, D., Tan, W., 2012. Biosensors and Bioelectronics 35, 475–478.

Qian, J., Ferguson, T.M., Shinde, D.N., Ramírez-Borrero, A.J., Hintze, A., Adami, C., Niemz, A., 2012. Nucleic Acids Research 40, e87.

Shao, Z., Liu, Y., Xiao, H., Li, G., 2008. Electrochemistry Communications 10, 1502–1504.

Sharon, E., Freeman, R., Riskin, M., Gil, N., Tzfati, Y., Willner, I., 2010. Analytical Chemistry 82, 8390–8397.

Shay, J., Bacchetti, S., 1997. European Journal of Cancer 33, 787–791.

Shay, J.W., Wright, W.E., 2002. Cancer Cell 2, 257–265.

Shlyahovsky, B., Li, D., Weizmann, Y., Nowarski, R., Kotler, M., Willner, I., 2007. Journal of the American Chemical Society 129, 3814–3815.

Wang, H., Wu, S., Chu, X., Yu, R., 2012a. Chemical Communications 48, 5916–5918.

Wang, J., Wu, L., Ren, J., Qu, X., 2012b. Small 8, 259–264.

Wege, H., Chui, M.S., Le, H.T., Tran, J.M., Zern, M.A., 2002. Nucleic Acids Research 31, e3.

Wu, L., Wang, J., Feng, L., Ren, J., Wei, W., Qu, X., 2012. Advanced Materials 24, 2447–2452.

Xiao, Y., Dane, K.Y., Uzawa, T., Csordas, A., Qian, J., Soh, H.T., Daugherty, P.S., Lagally, E.T., Heeger, A.J., Plaxco, K.W., 2010. Journal of the American Chemical Society 132, 15300–15307.

Xiao, Y., Pavlov, V., Niazov, T., Dishon, A., Kotler, M., Willner, I., 2004. Journal of the American Chemical Society 126, 7430–7431.

Yang, W., Zhu, X., Liu, Q., Lin, Z., Qiu, B., Chen, G., 2011. Chemical Communications 47, 7452–7454.

Zhang, Z., Sharon, E., Freeman, R., Liu, X., Willner, I., 2012. Analytical Chemistry 84, 4789–4797.

Zhang, Z., Zhang, C., 2012. Analytical Chemistry 84, 1623–1629.

Zhou, H., Liu, J., Xu, J.J., Chen, H.Y., 2011. Chemical Communications 47, 8358–8360.

Zhou, X., Xing, D., 2012. Chemical Society Reviews 41, 4643–4656.

Zhou, X., Xing, D., Zhu, D., Jia, L., 2008. Analytical Chemistry 81, 255–261.

Zuo, X., Xia, F., Patterson, A., Soh, H.T., Xiao, Y., Plaxco, K.W., 2011. ChemBioChem 12, 2745–2747.